Advanced Spectrum Management in Multicell OFDMA Networks Enabling Cognitive Radio Usage

F. Bernardo, J. Pérez-Romero, O. Sallent, R. Agustí
Department of Signal Theory and Communications
Universitat Politècnica de Catalunya (UPC)
Barcelona, Spain
[fbernardo, jorperez, sallent, ramon]@tsc.upc.edu

Abstract— **In this work, an approach to an Advanced Spectrum Management (ASM) framework in a multicell OFDMA network is given. The aim of this paper is to illustrate that an ASM operation over a multicell OFDMA scenario enables the efficient use of the available spectrum. Then, some spectrum bands could be released by primary or licensed spectrum holders in a geographical area to be shared with or rented to other secondary markets in a cognitive radio environment.**

Keywords- Advanced Spectrum Management; Multicell; OFDMA

I. INTRODUCTION

The regulatory perspective on how the spectrum should be allocated and utilized in future wireless scenarios is evolving towards a cautious introduction of more flexibility in spectrum management together with economic considerations on spectrum trading. This new spectrum management paradigm is driven by the growing competition for spectrum and the requirement that the spectrum is used more efficiently [1]. A broad view in that respect is to examine spectrum utilization from a time/location/band/power perspective as suggested in the Federal Communications Commission Spectrum Policy Task Force Report [2], where it was stated that the spectrum shortage results from the spectrum management policy rather than the physical scarcity of usable frequencies. Since then, this underutilization of spectrum has stimulated a great research interest in searching for better spectrum management policies and techniques [3][4].

In this framework, dynamic spectrum management strategies have been seen as effective approaches to use the available spectrum optimally in time and space among the different Radio Access Technologies (RATs) [5]. For this reason and to get a better spectral use, primary and secondary spectrum markets can be envisaged, so that primary operators release as much spectrum as possible to lease it to secondary markets.

The objective for the primary operators is to get the maximum spectral efficiency and profit from spectrum without degrading the satisfaction of the users. Then, in order to make attractive to primary operators renting their precious spectrum, the business model of the secondary market should be different from that of the primary operators (e.g., a cellular and a video broadcasting operator), so that they do not compete directly within the primary market. For example, the spectrum in the secondary market could be used in an infrastructure-less manner (e.g., opportunistic ad-hoc cognitive radio networks) so the secondary market is not using the primary spectrum permanently. The economic profit is clearly an incentive for the primary operators that will make profitable the investments made on acquiring the spectrum licenses.

To cope with that framework, it is important to have a flexible radio interface that enables a flexible spectrum management. OFDMA (Orthogonal Frequency Division Multiple Access) is the candidate technology for achieving that interface [6]. Typically, the radio resources in OFDMA RATs are divided in both time and frequency, building a time-frequency grid where the minimum radio resource that can be assigned is usually named as a *Resource Block* (RB). In frequency, the whole available bandwidth is divided into groups of adjacent subcarriers or *chunks* whereas in time it is divided into frames. Therefore, this flexible RAT should be exploited to get the desired objective of spectral efficiency.

Furthermore, a flexible chunk allocation mechanism that adapts to users' requirements is also desirable. In fact, the conventional schemes (e.g., reuse 1 where all chunks are assigned to all cells or reuse 3 where all chunks are distributed regularly between groups of 3 cells) are static since the allocation of frequency resources to cells is uniform and cannot be changed dynamically. This means that the frequency deployment cannot be adapted to nonhomogeneous spatial traffic distributions and their variation in time. Moreover, the application of advanced spectrum techniques such as spectrum pooling [7] or spectrum sharing [8] when using conventional schemes may be hard. That is, it is no easy to find a group of cells where the same set of chunks is not used to be offered to another spectrum holder.

In this paper we present a framework that constitutes a first step to ASM in a multicell OFDMA system. Specifically, a full Dynamic Spectrum Allocation (DSA) algorithm that considers the heterogeneous spatial traffic distributions to decide a proper chunk-to-cell assignment is presented. It is shown that the proposed scheme improves spectral efficiency, maintains users' satisfaction and allows releasing some frequency bands in large geographical areas, so that, e.g., they can be used for opportunistic spectrum access by cognitive secondary users.

The paper is organized as follows. The ASM framework is presented in section II, explaining the scheduling mechanisms and the dynamic algorithm proposed in this paper. Section III presents the simulation model while results obtained are shown in section IV. Finally, section V concludes this paper.

This work has been performed in the framework of the projects E3, which has received research funding from the Community's Seventh Framework programme, and COSMOS (TEC2004-00518). This paper reflects only the authors' views and the Community is not liable for any use that may be made of the information contained therein. The contributions of colleagues from E3 consortium as well as the Spanish Educational Ministry supporting FPU grant AP20051165 are hereby acknowledged.

II. ASM FRAMEWORK

The ASM framework presented in this paper is divided into two decision blocks. One is called Short-Term Scheduler (STS) and tries to exploit multiuser diversity due to fast frequency selective fading in the short-term. The other is denoted as ASM scheduler and provides the dynamic chunk-to-cell allocation in the system in the medium-long term. This scheduling architecture has also been reported in 3GPP [9] or in recent related work [10][11].

A. Short-Term Scheduler

The STS schedules the users served by a given cell in the time-frequency grid, by deciding which RBs are allocated to each user. Following the current trend of decentralizing functions towards edge network nodes, which enables shorter frame durations, lower latencies and higher speed channels, the STS would be located at the base station, e.g. the eNB (E-UTRAN NodeB) in the particular case of the architecture proposed for Long-Term Evolution (LTE) by 3GPP in [9].

Different policies can be followed by the STS for scheduling the users. For example, the users can be scheduled as function of the channel quality, the buffer delay, the throughput, the buffer occupancy, the service, etc. Thus, the STS is traffic and channel aware in its decisions, and tries to exploit the multiuser diversity on a frame by frame basis by making use of the available resources at each cell.

Several schemes of scheduling can be deployed and constitute a hot research topic nowadays [12][13]. Usually, Round Robin is employed, but its performance is poor since it assigns the channel cyclically to users and then is not channel aware in its decisions. Proportional Fair (PF) and Generalized Proportional Fair (GPF) have been proposed to provide a trade-off between fairness and system throughput and to exploit multiuser diversity in time [14]. GPF is a generalized version of PF where weights are introduced to change the trade-off between fairness and throughput. In addition, in [15], users are separately scheduled in each chunk. Then, not only multiuser diversity is exploited in time but also in frequency. The aim is that each RB of the time-frequency grid is given fairly to each user. Their scheduling decision is expressed as

$$m^*(t) = \arg\max_m \left\{ \frac{\left(R_{m,n}(t)\right)^\alpha}{\left(W_{m,n}(t)\right)^\beta} \right\} \quad (1)$$

where $m^*(t)$ is the user scheduled in the chunk n at frame t. $R_{m,n}(t)$ represents the instantaneous achievable rate that user m can get at chunk n in case the chunk is assigned to him/her. $W_{m,n}(t)$ is the window-averaged version of $R_{m,n}(t)$ as follows:

$$W_{m,n}(t) = (1 - \frac{1}{T_W}) W_{m,n}(t-1) + \frac{1}{T_W} \overline{R}_{m,n}(t-1) \quad (2)$$

where T_W is the window size in frames and $\overline{R}_{m,n}(t)$ stands for the final received rate at frame t after scheduling. The parameters $\alpha \geq 0$ and $\beta \geq 0$ are the weighting values for the GPF scheduler. The greater α and the lower β, the greater the probability of scheduling users with good channel condition and vice versa. PF is easily obtained by setting $\alpha=1$ and $\beta=1$.

B. ASM Scheduler

The ASM scheduler is in charge of deciding the chunks allocated to each cell by executing the DSA algorithm. It would be located in a network node with the ability to control a set of cells. The objective of this scheduling is to adapt the system to traffic variations in time and space in the medium-long term (i.e., minutes or hours) while maintaining users' satisfaction and avoiding intercell interference. Furthermore, it should try to achieve an efficient spectrum usage by releasing unnecessary frequency resources that can be used by e.g. secondary cognitive radio users. As an example, Figure 1 shows a general case where several primary operators coexist in a given geographical region. Thanks to ASM operation, these primary operators may share some spectrum bands with other secondary spectrum users exploiting opportunistic access to released pieces of spectrum.

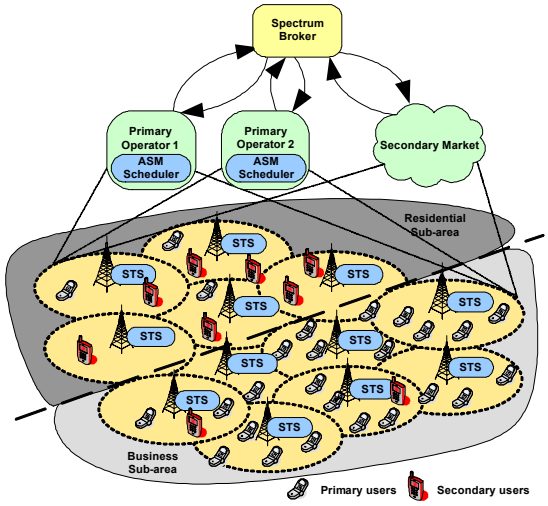

Figure 1. ASM framework architecture

Fig. 1 shows a hierarchical architecture, where each primary operator has its own ASM scheduler. There is a Spectrum Broker (SB) that manages the spectrum transactions between primary and secondary markets. The SB may belong to the legacy spectrum proprietary (e.g., the government) or perhaps it may be a third party in which operators trust.

Finally, the spatial distribution of the traffic may be different within the operation area. In Fig. 1 we can distinguish two subareas, one residential subarea and a business subarea. Traffic distribution in these subareas might not be correlated (e.g., very high traffic load may be experimented in the business subarea in the mornings and very a low one in residential subarea, while the opposite happens in the evenings). Therefore, traffic distribution changes not only temporally but also spatially in the long-term and the ASM scheduler tries to cope with these variations.

Inputs for the ASM scheduler come from each cell under its control and may include the mean delay experienced by users, the interference reported by the base stations, buffer status, etc. Also, static information such as the deployment of cells or frequency reuse schemes could be available.

Some of the system parameters that the ASM scheduler could change are the specific chunks allocated to each cell, the STS configuration parameters like thresholds, weights, etc. Then different cells are given different number of chunks depending on their traffic status. Furthermore, the location of the chunks within the system bandwidth is also taken into account in order to optimize a given indicator (e.g., intercell interference, outage probability, number of non-allocated chunks to a cluster of cells, etc.).

As a first step, in this paper we focus on the ASM operation of a single primary operator, which enables the future mechanisms needed for the scenario envisaged in Fig. 1.

C. Dynamic Spectrum Allocation (DSA) Algorithm

The ASM scheduler will run the DSA algorithm that will use the inputs and the outputs given above. In this paper, we have developed a DSA algorithm divided in two steps. First it computes the number of chunks to assign to a given cell. Then it decides which specific chunks are allocated. In the first step, the number of chunks is adapted to the cell load (i.e., number of users); so that high loaded cells get a higher number of chunks. Specifically, given a maximum number of chunks N available in the system, the number of chunks $N_j \in [1..N]$ allocated to the j-th cell is given by:

$$N_j = \min\left(N, \max\left(1, \left\lfloor f \frac{U_j \cdot T_{th}}{W/N \cdot \eta_{\max}} \right\rfloor \right) \right) \qquad (3)$$

where $\lfloor x \rfloor$ represents integer part and U_j are the users served by j-th cell, T_{th} represents the satisfaction throughput per user (i.e., the minimum throughput that a user may expect from the system to be satisfied), W is the total system bandwidth and W/N is then the chunk bandwidth, η_{max} stands for the maximum theoretical spectral efficiency in the system due to modulation in bps/Hz and f is an empirical margin factor. Equation (3) provides the required number of chunks that permits to achieve the total satisfaction throughput requested by the users in the cell.

As a second step, the chunks are allocated to each cell determining the potential intercell interference. Our algorithm takes into account the cell deployment and the load of the cells. That is, in order to improve the intercell interference, the chunk allocation is performed trying to avoid that neighboring cells use the same chunk. Also, if one cell is high loaded, cells around it should not re-use the same chunks since those chunks possibly generate interference all the time.

To take this into account, we construct a symmetric KxK matrix $\boldsymbol{A}$ (K is the number of cells), where $A(i,j)$ indicates the neighboring relationship between cells i and j in terms of loads and distances as in the following:

$$A(i,j) = \begin{cases} 0 & if\ i = j \\ \left(\frac{U_i}{U_j} + \frac{U_j}{U_i} \right) \left(\frac{R}{D_{ij}} \right)^{\delta} & otherwise \end{cases} \qquad (4)$$

where U_j stands for the load of cell j (i.e. number of users), R denotes the cell radius, D_{ij} is the distance from cell i to the border of cell j and δ is the propagation exponent. Then, matrix $\boldsymbol{A}$ is a coupling matrix based on cell distances and includes the ratio of loads between cells. Note that the term $A(i,j)$ includes the sum of load ratios ($U_i/U_j + U_j/U_i$) in order to obtain a symmetric matrix, considering that the mutual effect $A(i,j)$ should be equal to the mutual effect $A(j,i)$. Low values in $\boldsymbol{A}$ mean that the cost of assigning the same chunk to those cells is small, whereas high values in $A(i,j)$ indicate that it is not convenient to allocate the same chunks to cells i and j.

Fig. 2 shows the chunk allocation algorithm for j-th cell supposing that the algorithm has been run until cell j-1. It assigns to the j-th cell the chunks that have less impact or cost in the neighboring cells. The symbols used in the figure are defined in the box within it.

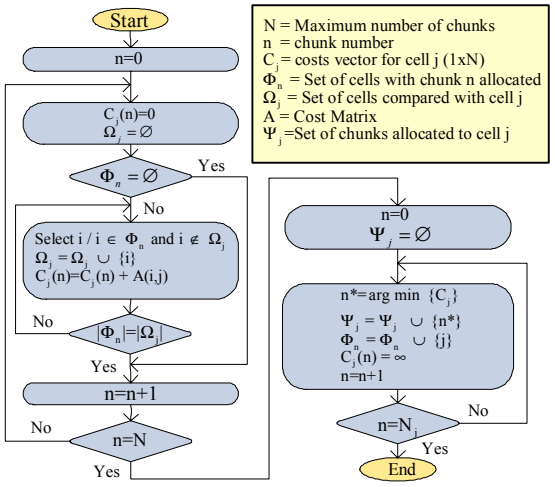

Figure 2. Step 2 of the DSA algorithm

III. Simulation Model

In this paper results for a downlink multicell scenario are obtained by means of dynamic simulations. The cellular scenario is composed of K=19 omnidirectional cells and its main parameters are collected in Table I. The total system bandwidth W is 4.5MHz and is divided into N=12 chunks that is a number big enough to provide frequency diversity. Path loss and large scale fading is considered flat for all the chunks while fast frequency selective fading may vary from one chunk to another depending on users' speed. Within a chunk, all the subcarriers present the same propagation features in terms of both fast and flat fading.

The power devoted to every chunk is constant and does not change during simulation (there is no power control). Then, the Signal to Interference plus Noise (SINR) ratio per each chunk is calculated as

$$\gamma_{m,n,i} = \frac{P_i G_{i,m} S_{i,m} F_{i,m,n}}{\sum_{\substack{j \in \Phi_n \\ j \neq i}} \left(P_j G_{j,m} S_{j,m} F_{j,m,n} \right) + P_N} \qquad (5)$$

where $\gamma_{m,n,i}$ represents the SINR in the n-th chunk for the m-th user in the serving cell i, and index j represents any interfering cell taken from the set of cells using the n-th chunk (denoted as Φ_n). P stands for the transmitted chunk power including trans-

mitter and receiver antenna gains. G denotes the distance dependant channel gain (inverse of path loss), S the large scale fading (shadowing) and F the fast frequency selective fading component that depends on the chunk n. It can be seen that F is considered for both the serving and the Φ_n interfering cells at chunk n. Note that G, S and F is computed for each user and cell. Lastly, P_N denotes the total noise power including receiver noise figure.

Despite there is no power control, users' transmission rate is variable by means of Adaptive Coding and Modulation (ACM). The achievable user rate is computed for each chunk as follows [16]:

$$R_{m,n,i} = \frac{W}{N}\log_2\left(1-\frac{1.5\gamma_{m,n,i}}{\ln(5BER)}\right) \quad (6)$$

where $R_{m,n,i}$ is the m-th user's rate in chunk n at cell i. BER stands for the target Bit Error Rate and should be BER<(1/5)exp(-1.5) ≈ 4.46%. In addition, this equation is valid for $\gamma_{m,n} < 30$ dB. It is supposed that perfect channel state information is available at both the transmitter and receiver sides.

The STS employed is a PF scheduler [15] that allocates RBs to users. Only one user is scheduled per chunk in each frame although a user can get more than one chunk per frame. Users are deployed in the scenario with always full loaded buffers. This means that a user always has information to transmit and then, he/she tries to get as much capacity as possible and is satisfied if the final throughput over the last second is above the satisfaction throughput T_{th}.

Load is distributed heterogeneously among cells in the scenario to prove that the DSA algorithm adapts to cells' loads and to enable the releasing of spectrum in the less loaded regions. Then, different system loads varying from U=30 to U=400 users were simulated.

The spatial distribution of the users taken for simulations and results is shown in Fig. 3, where P_r indicates the fraction of the U users assigned to each cell. Moreover, users are uniformly distributed within a cell and their mobility is restricted to the cell where they belong to.

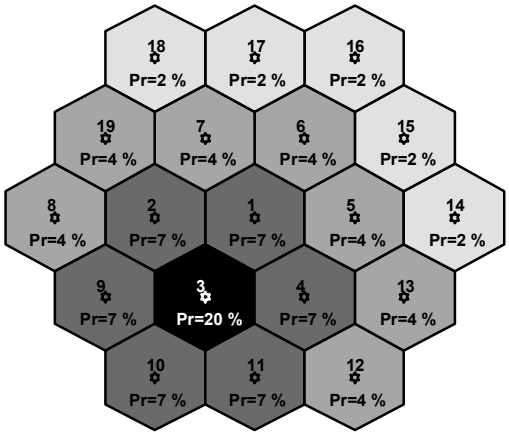

Figure 3. Spatial distribution of the users in the scenario. Cells with higer load are depicted with dark gray, and low loaded cells with bright gray.

TABLE I SIMULATION PARAMETERS

Number of cells	K = 19
Cell Radius	R = 500 m
Number of antennas	1 Tx, 1 Rx
Antenna Patterns	Omnidirectional
Power per chunk	P = 32.22 dBm
Carrier Frequency	2 GHz
Total Bandwidth	W = 4.5 MHz
Number of chunks	N = 12
Number of Subcarriers per chunk	25
Chunk bandwidth	W/N = 375 kHz
Frame duration	2 ms
Path Loss at d Km	128.1+37.6log10(d) in dB
Shadowing	Lognormal Distribution
Standard deviation	σ=8 dB
De-correlation model	[6]
De-correlation distance	50m
Small Scale Fading Model	[6]
UE thermal noise	-174 dBm/Hz
UE noise factor	9 dB
UE speed	50 km/h
User's satisfaction throughput	T_{th} = 128 kb/s
Maximum theoretical spectral efficiency	η_{max} = 4 bits/s/Hz
Margin factor	f = 2
BER	10^{-3}
Scheduling	Proportional Fair
Averaging Window size	T_w = 50 frames

IV. RESULTS

Results are presented in terms of average number of chunks allocated per cell, spectral efficiency, users' dissatisfaction probability and spectrum usage per cell. Two classic fixed Frequency Reuse Factor (FRF) schemes are compared with the DSA-128 algorithm (DSA algorithm considering a satisfaction throughput threshold equal to 128kbps). These are FRF1 that assigns all available chunks to all cells and FRF3 where the bandwidth is divided in 3 subbands and each subband is assigned to a cell within a cluster of three cells. Then the same frequency pattern is reused regularly once each 3 cells.

The average number of chunks per cell is depicted in Fig. 4. It can be seen the adaptability of the DSA-128 algorithm, that increases the number of chunks per cell with the increasing load. Differently from FRF1 and FRF3, DSA-128 is allocating wisely the required number of chunks to assure the minimum user throughput above satisfaction threshold. Then, unnecessary chunks will be available to be pooled, released and accessed by secondary users.

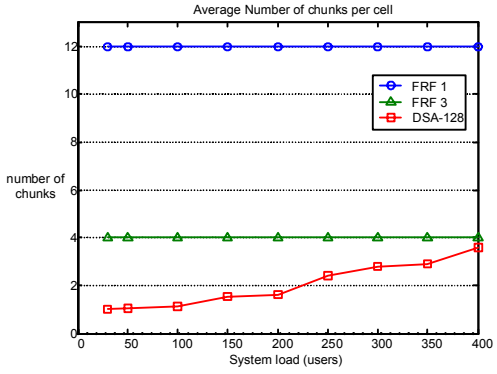

Figure 4. Average number of chunks per cell

Spectral efficiency η is calculated as:

$$\eta = \frac{Total\ cell\ throughput}{Cell\ Bandwidth} \quad \text{bits/s/Hz} \tag{7}$$

Fig. 5 shows the average spectral efficiency per cell, where it can be seen that DSA-128 clearly outperforms FRF1 and FRF3, especially for low loads, where the number of chunks needed to satisfy users' requirements is low. In that case, the DSA-128 algorithm is able to find a proper allocation of the chunks to cells that reduces the intercell interference, and then the throughput achieved per cell is increased. This together with the low number of chunks allocated to each cell achieves a better usage of spectrum. Logically, for the DSA-128 the spectral efficiency decreases with the increasing load since the allocated number of chunks per cell also increases.

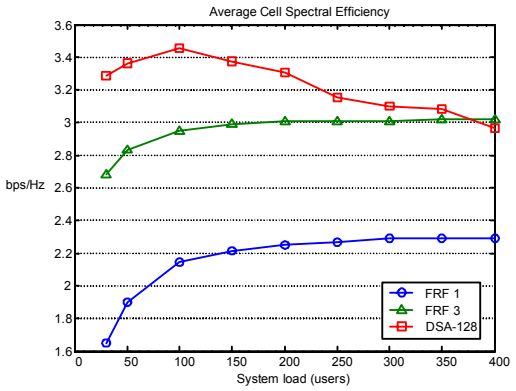

Figure 5. Average cell spectral efficiency

Fig. 6 shows the dissatisfaction probability (the probability that the average throughput of the users in the system during one second is lower than T_{th}=128kbps). Note that DSA-128 follows the same tendency than FRF1 and is the best scheme for high loads. However FRF3 shows very poor performance since the number of allocated chunks per cell (N/3) is not high enough to guarantee users' satisfaction throughput. Then although FRF3 reduces the intercell interference and achieves greater spectral efficiency than FRF1, it is not able to maintain users' satisfaction. Therefore, Fig. 5 and Fig. 6 clearly show that DSA is the best adapted scheme since it is able to increase system's spectral efficiency while maintaining user's satisfaction.

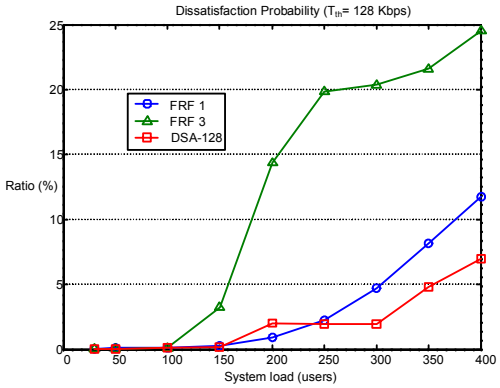

Figure 6. Dissatisfaction probability

Furthermore, it has been said that DSA permits to release spectrum in a region by pooling frequency resources. To measure the spectrum usage per cell and to see graphically the capacity of releasing spectrum in a given band we have introduced a new metric called Regional Spectrum Usage (RSU). RSU is defined per cell and for a band composed of a set of B chunks as follows:

$$RSU_j^{(B)} = \frac{1}{|B|}\sum_{n\in B} u_{jn} \tag{8}$$

where u_{jn} is the chunk usage for cell j over chunk n defined as

$$u_{jn} = \begin{cases} 1 & \text{if cell } j \text{ uses chunk } n \\ \dfrac{\left|\Phi_n^{\mathcal{C}_j}\right|}{\left|\mathcal{C}_j\right|} & \text{otherwise} \end{cases} \tag{9}$$

where $\mathcal{C}_j$ represents the set of first ring neighboring cells of j, and $\Phi_n^{\mathcal{C}_j}$ is the set of cells that use the n-th chunk within $\mathcal{C}_j$. Therefore, $RSU_j^{(B)}$ denotes the spectrum usage over a band of B chunks in cell j and takes into account the usage in the neighboring cells on the chunks not used by cell j. Note that $RSU_j^{(B)} \in [0,1]$. $RSU_j^{(B)}=1$ means that band B is completely used in j and/or in $\mathcal{C}_j$ whereas zero means that the band is completely free. Thus, the lower the $RSU_j^{(B)}$, the easier that band B can be released in a region around cell j.

Table II includes the system's average RSU for the whole bandwidth (i.e., B=W). FRF1, FRF3 and DSA for several loads and a satisfaction throughput of 128kbps are compared. It can be seen that in the case of DSA, the usage of the spectrum is more efficient (i.e. lower values of RSU) than in the other two reuses, showing that DSA adapted the number of chunks per cell to the users' satisfaction requirements and then the unnecessary spectrum is available to be released.

TABLE II SYSTEM AVERAGE RSU

FRF1	1
FRF3	0.67
DSA 30 users	0.17
DSA 100 users	0.19
DSA 200 users	0.28
DSA 300 users	0.45
DSA 400 users	0.55

Finally, as an illustrative example, Fig. 7 shows the RSU map in the system for different loads and a band B from chunks 9 to 12 (1.5 MHz bandwidth). The RSU map is always the same for FRF1 FRF3 since they deploy the chunks regardless the cells' load. Cells with RSU < 30% are depicted with a triangle. In these cells, at least 70% of band B is free for releasing to secondary markets. Note that DSA not only outperforms the other reuse schemes in number of triangles, it also allows finding a cluster of contiguous cells where that band has a low utilization.

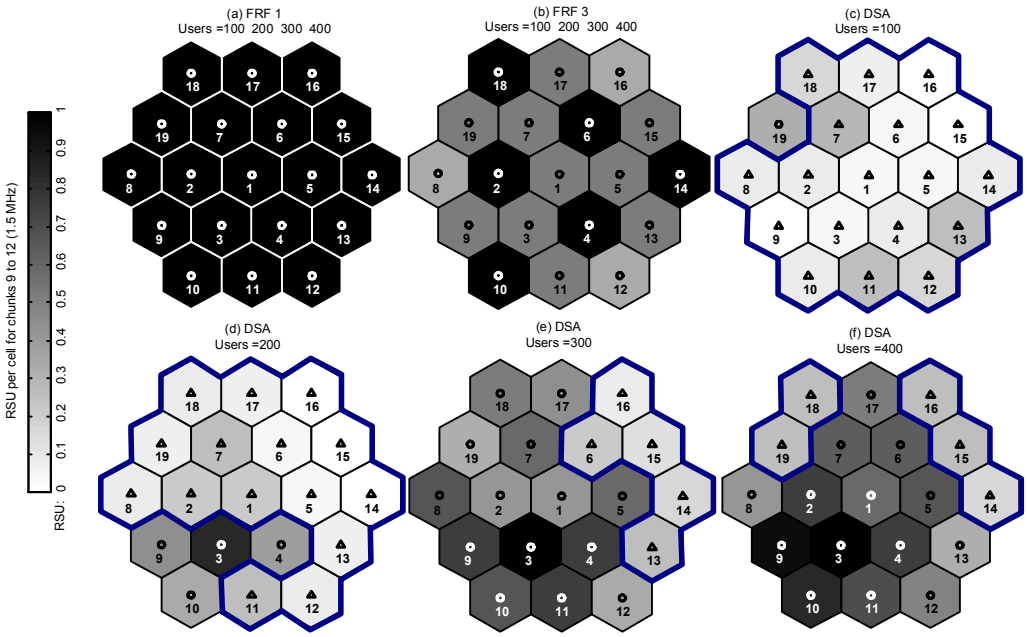

Figure 7. Regional Spectrum Usage per cell for chunks 9 to 12 and for FRF1 (a), FRF3 (b) , and DSA (c,d,e,f)

It is important to see that for loads below 200 users the band is almost free in the whole scenario. Therefore, within an ASM framework, spectrum could be released in large geographical areas, which enables the deployment of more complex secondary cognitive networks within those areas.

V. CONCLUSION

In this work, an approach to an Advanced Spectrum Management (ASM) framework in a multicell OFDMA network has been given. Within this framework, a dynamic chunk reuse allocation algorithm has been presented. It improves overall system's spectral efficiency while maintains users' satisfaction. Also it has been shown that DSA could release some spectrum bands in large geographical areas so that this spectrum will not be wasted and could be exploited by secondary cognitive users. This property makes the dynamic reuse very suitable for future wireless networks because spectrum is a scarce and expensive resource that will be used in a more efficient way, satisfying primary users' needs and making room for opportunistic secondary users.

REFERENCES

[1] J. A. Hoffmeyer, "Regulatory and standardization aspects of DSA technologies – Global Requirements and Perspectives", IEEE 1st DySPAN, pp.700-705, 8-11 Nov. 2005

[2] FCC Spectrum Policy Task Force, "Report of the spectrum efficiency working group," Nov. 2002. [on-line] at http://www.fcc.gov/sptf/reports.html

[3] Q. Zhao, B. M. Sadler, "A survey of dynamic spectrum access: signal processing, networking, and regulatory policy", IEEE Signal Processing Magazine, Vol. 24, pp. 79 – 89 May 2007

[4] OFCOM, Cognitive radio technology, a study for OFCOM, [on-line] http://www.ofcom.org.uk/research/technology/overview/emer_tech/cograd/cograd_main.pdf

[5] P. Leaves, K. Moessner, R. Tafazolli, D. Grandblaise, D. Bourse, R. Tönjes, M. Breveglieri, "Dynamic spectrum allocation in composite reconfigurable wireless networks", IEEE Communications Magazine, vol. 42, pp. 72-81, May 2004.

[6] 3GPP, TR 25.814 v7.1.0, "Physical layer aspects for evolved Universal Terrestrial Radio Access (UTRA)", Release 7, Sep. 2006.

[7] T.A. Weiss, F.K. Jondral, "Spectrum pooling: an innovative strategy for the enhancement of spectrum efficiency", IEEE Communications Magazine, vol. 42, pp. 8- 14, Mar. 2004

[8] J.M. Peha, "Approaches to spectrum sharing" IEEE Communications Magazine, vol. 43, pp. 10- 12, Feb. 2005

[9] 3GPP, TR 25.912 v7.1.0, "Feasibility study for evolved Universal Terrestrial Radio Access (UTRA) and Universal Terrestrial Radio Access Network (UTRAN)", Release 7, 2006.

[10] G. Li, H. Liu, "Downlink radio resource allocation for multicell OFDMA system", IEEE Trans. on Wireless Communications, vol. 5, pp. 3451-3459, Dec. 2006

[11] D. Astely, E. Dahlman, P. Frenger, R. Ludwig, M. Meyer, S. Parkvall, P. Skillermark, N. Wiberg, "A future radio-access framework" IEEE JSAC, vol. 24, pp. 693-706, Mar. 2006

[12] S. Ko, J. Heo, K. Chang, "Aggressive subchannel allocation algorithm for efficient dynamic channelallocation in multiuser OFDMA system", 17th annual IEEE PIMRC'06, pp. 1-5. 2006.

[13] A. Pokhariyal, T.E. Kolding, P.E. Mogensen, "Performance of downlink frequency domain packet scheduling for the UTRAN long term evolution", 17th annual IEEE PIMRC'06, pp. 1-5. 2006.

[14] A. Jalali, R. Padovani, R. Pankaj, "Data throughput of CDMA-HDR a high efficiency-high data rate personal communication wireless system" IEEE 51st VTC 2000-Spring Tokyo. Vol.3, pp. 1854-1858

[15] C. Wengerter, J. Ohlhorst, A.G.E. von Elbwart, "Fairness and throughput analysis for generalized proportional fair frequency scheduling in OFDMA", IEEE 61st VTC 2005-Spring. Vol. 3, pp. 1903-1907 Jun. 2005

[16] J. Jang, K.B. Lee, "Transmit power adaptation for multiuser OFDM systems" IEEE JSAC, Vol. 21, pp. 171- 178, Feb. 2003